

Liquid Water from First Principles: Investigation of Different Sampling Approaches

I-Feng W. Kuo,[†] Christopher J. Mundy,[†] Matthew J. McGrath,^{†,‡} J. Ilja Siepmann,^{*,†,‡} Joost VandeVondele,[§] Michiel Sprik,[§] Jürg Hutter,^{||} Bin Chen,[⊥] Michael L. Klein,[#] Fawzi Mohamed,[∇] Matthias Krack,[∇] and Michele Parrinello[∇]

Chemistry and Materials Science Directorate, Lawrence Livermore National Laboratory, Livermore, California 94550, Departments of Chemistry and of Chemical Engineering and Material Science, University of Minnesota, 207 Pleasant Street SE, Minneapolis, Minnesota 55455-0431, Department of Chemistry, University of Cambridge, Lensfield Road, Cambridge CB2 1EW, United Kingdom, Physical Chemistry Institute, University of Zurich, Winterthurerstrasse 190, CH-8057 Zurich, Switzerland, Department of Chemistry, Louisiana State University, Baton Rouge, Louisiana 70803-1804, Center for Molecular Modeling and Department of Chemistry, University of Pennsylvania, 231 South 34th Street, Philadelphia, Pennsylvania 19104-6323, and Laboratory of Physical Chemistry, ETH Zurich, USI-Campus, Via Giuseppe Buffi 13, CH-6904 Lugano, Switzerland

Received: May 21, 2004; In Final Form: July 6, 2004

A series of first principles molecular dynamics and Monte Carlo simulations were carried out for liquid water to investigate the reproducibility of different sampling approaches. These simulations include Car–Parrinello molecular dynamics simulations using the program CPMD with different values of the fictitious electron mass in the microcanonical and canonical ensembles, Born–Oppenheimer molecular dynamics using the programs CPMD and CP2K in the microcanonical ensemble, and Metropolis Monte Carlo using CP2K in the canonical ensemble. With the exception of one simulation for 128 water molecules, all other simulations were carried out for systems consisting of 64 molecules. Although the simulations yield somewhat fortuitous agreement in structural properties, analysis of other properties demonstrate that one should exercise caution when assuming the reproducibility of Car–Parrinello and Born–Oppenheimer molecular dynamics simulations for small system sizes in the microcanonical ensemble. In contrast, the molecular dynamics and Monte Carlo simulations in the canonical ensemble appear to be more reliable. Furthermore, in the case of canonical Car–Parrinello molecular dynamics simulations the application of Nosé–Hoover chain thermostats allows the use of larger fictitious electron masses. For the Becke–Lee–Yang–Parr exchange and correlation energy functionals and norm-conserving Troullier–Martins or Goedecker–Teter–Hutter pseudopotentials, these simulations at a fixed density of 1.0 g/cm³ and a temperature close to 315 K point to an overstructured liquid with a height of the first peak in the oxygen–oxygen radial distribution function of about 3.0, an underestimated value of the classical constant-volume heat capacity of about 70 J/(mol K), and an underestimated self-diffusion constant of about 0.04 Å²/ps.

I. Introduction

Water holds a unique role among liquids, not only because of its ubiquity and importance on earth but also because of its anomalous liquid properties. Thus, understanding its properties has been a grand challenge for liquid state theory¹ and molecular simulation.² The first particle-based simulations of liquid water using pairwise empirical potentials were carried out almost 40 years ago.³ However, the strong dipole moment and large polarizability of water and its participation in many chemical processes, particularly its self-dissociation, pose a challenge for empirical potentials. Although great strides have been made in the development of empirical force fields for water, none of these has yet succeeded to yield a quantitative description of the thermodynamic, structural, and dynamic properties of water

over its entire liquid range.⁴ In contrast, an ab initio representation of water affords the opportunity to study both physical and chemical properties of water.

The first Car–Parrinello molecular dynamics (CPMD) simulation⁵ for liquid water employing a quantum-mechanical description of the molecular interactions was performed in the early nineties,⁶ but available computer resources limited this CPMD simulation to a small system size (32 molecules) and short simulation length (1.5 and 2 ps for equilibration and production, respectively). However, it should be emphasized that without the gains in efficiency afforded by the CPMD approach,⁵ which propagates the electron density using classical dynamics using a fictitious electron mass, μ with unit of energy \times (time)², first principles simulations for liquid water would not have been possible in the early nineties.

Large increases in the available computer power and in the efficiency of the simulation approaches are now enabling more systematic studies of the liquid properties of water using first principles approaches. In particular, using the CPMD approach, it is now possible to follow the trajectories of 64 water molecules for more than 10 ps^{7–9} or of 216 water molecules for about 5 ps.¹⁰ Thus, one should expect that the field of first principles

* Corresponding author. E-mail: siepmann@chem.umn.edu.

[†] Lawrence Livermore National Laboratory.

[‡] University of Minnesota.

[§] University of Cambridge.

^{||} University of Zurich.

[⊥] Louisiana State University.

[#] University of Pennsylvania.

[∇] ETH Zürich.

simulations of water has matured in the 10 years following the initial simulation.⁶ However, two independent reports by Asthagiri et al.¹¹ and Grossman et al.¹² have recently questioned the reproducibility of previous first principles simulations for liquid water. Asthagiri et al. suggested that different analysis procedures, different choices of the fictitious electron masses, or different thermostating procedures "could play a role ... in the prevailing nonuniform agreement of the simulation results".¹¹ Grossman et al.¹² evaluated among other parameters explicitly the dependence of structural and dynamic properties on the fictitious electron mass and for a relatively small value of $\mu = 340$ au obtained a liquid phase that is significantly more structured than seen in previous simulations.⁷⁻⁹

In light of the recent reports, the goal of this research is to further assess the reproducibility of first principles simulations of liquid water using different approaches to sample the trajectories (e.g. different electronic structure methods, different fictitious electron masses, and different statistical mechanical ensembles), but maintaining the other simulation parameters (density functional and to the extent possible temperature). The next section provides a brief description of the simulation details and analysis parameters, and in the following section the results are presented and discussed.

II. Simulation Methods and Details

The first principle simulations of this work were performed using the computer programs CPMD and CP2K that are developed by a large group of researchers and are publicly available.^{13,14} Car-Parrinello molecular dynamics⁵ combines density functional theory with extended systems molecular dynamics¹⁵ via the introduction of a fictitious electronic kinetic energy term into the Lagrangian. This classical treatment of the electronic degrees of freedom allows for a very efficient sampling of the Kohn-Sham energy functional¹⁶ for soft-condensed matter systems, but requires the use of a fictitious electron mass, μ , as a parameter of the Lagrangian that needs to be chosen judiciously to allow for the adiabatic separation of nuclear and electronic degrees of freedom.¹⁷ Furthermore, the use of separate Nosé-Hoover chain thermostats^{18,19} for the ionic and electronic degrees of freedom enables CPMD to control the adiabatic separation for first principles simulations in the canonical ensemble.²⁰ The computer program CPMD also allows one to sample molecular dynamics trajectories using Born-Oppenheimer dynamics, i.e., quenching the electronic structure at every time step.²¹

The program CP2K¹⁴ is a general purpose program that builds upon the success of CPMD. The electronic structure part of CP2K, called QUICKSTEP, uses the Gaussian plane wave (GPW) method²² for the calculation of forces and energies. The GPW method is based on the Kohn-Sham formulation¹⁶ of density functional theory and employs a hybrid scheme of Gaussian and plane wave functions. Here the Kohn-Sham orbitals are expanded using a linear combination of atom-centered Gaussian-type orbital functions, and an auxiliary basis set of plane waves describes the electronic charge density.²² This combination is chemically more intuitive and computationally more efficient than the sole use of a plane wave basis set. First principles simulations with CP2K sample directly from the Born-Oppenheimer surface.

The computational efficiency of the GPW energy routine is exploited in CP2K-MC, a module of CP2K that allows for Monte Carlo sampling from various statistical-mechanical ensembles,² including those with fluctuating particle numbers. Use of a Monte Carlo framework is advantageous because temperature,

pressure, and chemical potential are explicitly accounted for in the acceptance rules,² and the momentum part of the Hamiltonian can be removed by integration;²³ i.e., the configurational properties are independent of any choice of mass. Our Monte Carlo implementation for water in the canonical ensemble employs three different types of trial moves: (i) translations of rigid molecules, (ii) rigid-body rotations around the molecular center of mass, and (iii) conformational moves altering either bond length or angle. The type of move is selected at random and the separate move types ensure equipartition of the translational, rotational, and vibrational degrees of freedom of the system. Presampling of trajectories^{24,25} with an inexpensive approximate potential²⁶ for a short sequence of moves is carried out to reduce the number of expensive ab initio energy evaluations, thereby enhancing the computational efficiency. The current implementation uses a sequence of 16 presampling moves per GPW energy calculation, resulting in an acceptance rate of 25% per presampling sweep (with maximum displacements that yield a 50% acceptance rate for the presampling moves). The length of the Monte Carlo simulations is measured in MC cycles, where one cycle consists of N GPW calculations (with $N = 64$ being the number of molecules), but it should be noted that one of these cycles encompasses about $2N$ accepted trial displacements; that is 4 times more than in a conventional simulation without presampling.

Table 1 summarizes the details for the eleven simulation runs for liquid water carried out for this work. The choices of BLYP density functional with generalized gradient approximation,²⁷ norm-conserving Troullier-Martins pseudopotential²⁸ with Kleinman-Bylander transformation to fully nonlocal form,²⁹ and plane wave cutoff, $c_{\text{PW}} = 85$ Ry for the Kohn-Sham orbitals follow those used in previous CPMD simulations for water.^{7,8} Two different choices for the fictitious electron mass were employed in some of the runs: a relatively low value of $\mu = 400$ au and a high value of $\mu = 800$ au that is at the upper end of values used previously for liquid H₂O (μ can be increased by a factor of $\sqrt{2}$ for simulations of D₂O). In the CP2K simulations, the norm-conserving pseudopotentials of Goedecker et al. (GTH)³⁰ were applied to remove the core electrons, a triple- ζ valence basis set augmented with two sets of d-type or p-type polarization functions (TZV2P) optimized for the use with the GTH pseudopotentials was employed for O and H, and a charge density cutoff of 280 Ry was used for the auxiliary plane wave basis set. The runs presented here were carried out on state-of-the-art parallel computers using between 64 and 288 processors, and the total amount of processor time required to complete the eleven simulation runs was on the order $\mathcal{O}(10^4)$ processor days.

It is well-known that the range of stable liquid densities increases as the temperature is increased away from the triple point and that strongly associating fluids are more prone to glassy behavior.¹ Therefore, a slightly elevated target temperature of 315 K was used here to reduce the risk that our simulations fall outside the liquid-phase range for the BLYP density functional.

Run CPMD-NVE-400 was started from the final configuration of a previous simulation of 64 water molecules (supercell of $L = 12.42$ Å) that used a smaller value of c_{PW} ,¹⁰ and was continued with $c_{\text{PW}} = 85$ Ry for 32 ps. Runs CPMD-NVE-BO, CPMD-NVE-800, CPMD-NVT-i-400, and CPMD-NVT-ie-800 and the first MC run CP2K-MC-NVT-1 were initialized from a configuration taken after the initial 6 ps of run CPMD-NVE-400. The same configuration was used to spawn three CP2K-MD-NVE runs but using slightly different values for the size of the

TABLE 1: Simulation Details for the Different Runs^a

	functional	basis set	pseudopotential	cutoff (Ry)	μ (au)	N	molecule	L (Å)	Δt (fs)
CPMD-NVE-BO	BLYP	PW	TM	85	n/a	64	D ₂ O	12.42	0.48
CP2K-MD-NVE-1	BLYP	TZV2P	GTH	280	n/a	64	H ₂ O	12.40	0.5
CP2K-MD-NVE-2	BLYP	TZV2P	GTH	280	n/a	64	H ₂ O	12.42	0.5
CP2K-MD-NVE-3	BLYP	TZV2P	GTH	280	n/a	64	H ₂ O	12.44	0.5
CPMD-NVE-400	BLYP	PW	TM	85	400	64	H ₂ O	12.42	0.097
CPMD-NVE-400-128	BLYP	PW	TM	85	400	128	H ₂ O	15.64	0.097
CPMD-NVE-800	BLYP	PW	TM	85	800	64	H ₂ O	12.42	0.097
CPMD-NVT-i-400	BLYP	PW	TM	85	400	64	H ₂ O	12.42	0.097
CPMD-NVT-ie-800	BLYP	PW	TM	85	800	64	H ₂ O	12.42	0.097
CP2K-MC-NVT-1	BLYP	TZV2P	GTH	280	n/a	64	H ₂ O	12.42	n/a
CP2K-MC-NVT-2	BLYP	TZV2P	GTH	280	n/a	64	H ₂ O	12.42	n/a

^a CPMD and CP2K denote the computer programs. MD, MC, NVE, and NVT refer to simulations using molecular dynamics or Monte Carlo in the microcanonical or canonical ensemble, respectively. The labels “i” and “ie” stand for the use of Nosé–Hoover chain thermostats with chain length $M = 3$ and using a seventh-order Yoshida–Suzuki integrator^{19,20} for only the ionic degrees of freedom ($\omega_{\text{ion}} = 3800 \text{ cm}^{-1}$; $T_{\text{ion}}^{\text{target}} = 315 \text{ K}$; with a separate chain for every ionic degree of freedom) or separately for ionic and electronic degrees of freedom ($\omega_{\text{ion}} = 2000 \text{ cm}^{-1}$; $T_{\text{ion}}^{\text{target}} = 315 \text{ K}$; $\omega_{\text{elec}} = 10\,000 \text{ cm}^{-1}$; $E_{\text{kinetic}}^{\text{target}} = 0.04 \text{ au}$; with a single Nosé–Hoover chain using an effective number of degrees of freedom equal to 6 times the number of electronic states), respectively. BO, the first number, and the second number denote Born–Oppenheimer dynamics, the value of μ for CPMD dynamics, and the number of molecules when different from $N = 64$, respectively. The numbers at the end of the names for the CP2K simulations denote different initial configurations (see text). BLYP, PW, TZV2P, TM, and GTH stand for Becke exchange plus Lee–Yang–Parr correlation functional,²⁷ a plane wave basis set, a triple- ζ valence basis set augmented with two sets of d-type or p-type polarization functions, and norm-conserving Troullier–Martins and Goedecker–Teter–Hutter pseudopotentials,^{28,30} respectively. The column labeled “cutoff” lists the plane wave and charge density cutoff for CPMD and CP2K runs, respectively. L and Δt are the length of the supercell and the time step, respectively.

supercell (see Table 1). The second MC run CP2K-MC-NVT-2 was initialized from the final configuration (32 ps) of run CPMD-NVE-400. Run CPMD-NVE-400-128 was started from a well equilibrated classical Monte Carlo simulation using the force field of Izvekov et al.²⁶ The total lengths of the molecular dynamics simulations ranged from 15 to 18 ps (with the exception of the longer run CPMD-NVE-400), and the total lengths of the two CP2K-MC-NVT runs ranged from 700 to 900 Monte Carlo cycles. In the four simulations using Born–Oppenheimer dynamics, CPMD-NVE-BO and CP2K-MD-NVE-*, the energy was converged to 10^{-11} au/atom at every step and the total energy was conserved over 10 ps to better than 1 part in 10^5 .

The analysis of the simulation data was carried out using the last 10 ps of the molecular dynamics trajectories (with the exception of 20 ps for run CPMD-NVE-400) and the last 500 cycles for the Monte Carlo runs. The radial distribution functions (RDFs) were calculated using a bin width of 0.005 Å for separations smaller than 1.2 Å (only including the intramolecular oxygen–hydrogen bond) and a bin width of 0.02 Å for larger separations. The coordination numbers were evaluated from the value of the oxygen–oxygen number integral at the position of the first minimum in the corresponding RDF. The classical constant-volume heat capacities were calculated from the fluctuations²³ either of the total energy for molecular dynamics runs in the canonical ensemble or of the potential energy for the Monte Carlo simulations to which the classical contribution of the momentum part was added. Finally, the self-diffusion constants for the MD simulations in the microcanonical ensemble were computed via the Einstein relation from linear fits to the diffusive regime (using a range from 2 to 7 ps) of the center-of-mass mean square displacements that were averaged by shifting the time origin by 1 ps. The statistical uncertainties given here were estimated from the variance of all 64-molecule simulations for which a given property was calculated (e.g., nine simulations for the structure data, but only four and six for the heat capacity and self-diffusion constant, respectively).

III. Results and Discussion

Before analyzing the trajectory of any simulation, one first needs to check for shortcomings in the sampling procedure and

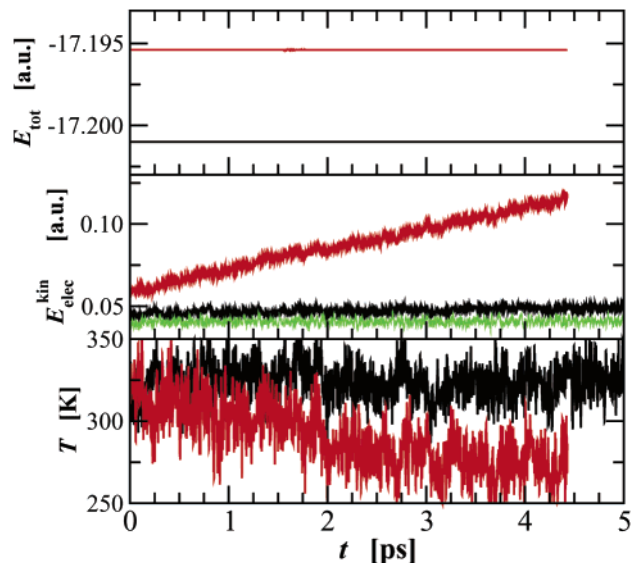


Figure 1. Comparison of the total energy per molecule (top panel), fictitious electronic kinetic energy (middle panel), and kinetic temperature of the ions (bottom panel). The results for runs CPMD-NVE-800 and CPMD-NVE-400-128 are shown as red and black lines, respectively. In addition, the behavior of the fictitious electronic energy of run CPMD-NVT-ie-800 is shown as a green line.

to assess whether the calculated properties show a drift or the appropriate fluctuation. One simulation, run CPMD-NVE-800, was aborted after a brief sampling period because this microcanonical simulation with the large fictitious electron mass did not result in adiabatic sampling. Figure 1 shows a comparison of the energetics of runs CPMD-NVE-800 and CPMD-NVE-400-128. It should be emphasized that monitoring the conservation of the total energy is not a very good diagnostic of whether a CPMD simulation achieves adiabatic sampling; e.g. the total energy of run CPMD-NVE-800 changed by less than 1 part in 10^6 over the 4.4 ps length of the simulation. A much better measure is the stability of the kinetic energy of the fictitious electronic degrees of freedom (or the magnitude of the force acting on the electron coefficients), and it shows the problems of run CPMD-NVE-800 very clearly (see Figure 1). Thus, any CPMD simulation in the microcanonical ensemble for H₂O using

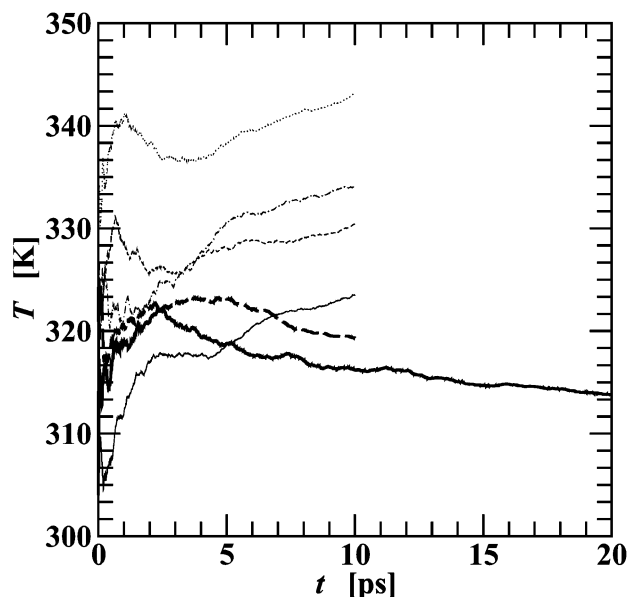


Figure 2. Comparison of the cumulative averages of the ionic temperature observed over the analysis parts of the simulations in the microcanonical ensemble. It should be noted that a change of 10 K in the ionic temperature is equivalent to a change in the corresponding kinetic energy per ion of less than 10^{-4} au. The results for the BOMD runs CPMD-NVE-BO, CP2K-MD-NVE-1, CP2K-MD-NVE-2, and CP2K-MD-NVE-3, are shown as thin solid, dashed, dotted, and dash-dotted lines, respectively, and for the CPMD runs CPMD-NVE-400 and CPMD-NVE-400-128 as thick solid and dashed lines, respectively.

an electron mass of about 800 au (or 1100 au for D_2O) should be suspect without an explicit demonstration that the electronic kinetic energy does not drift significantly throughout the continuous run. Furthermore, the limit of what constitutes a sufficiently small electronic mass for a simulation in the microcanonical ensemble depends on molecule type (e.g., H_2O versus D_2O), temperature (larger ion mobility requires smaller μ), and length of the run. The drift in the fictitious electronic kinetic energy per molecule over a 4 ps trajectory in runs CPMD-NVE-400 and CPMD-NVE-400-128 is about a factor of 30 smaller than for run CPMD-NVE-800. Thus, the suitable choice of μ would require reevaluation once CPMD simulations for water are targeted to reach the hundred picosecond range. Finally, the drift in the fictitious electronic kinetic energy for run CPMD-NVT-ie-800 is smaller by factors of 300 and 10 than those for runs CPMD-NVE-800 and CPMD-NVE-400, respectively. Thus, the use of Nosé–Hoover chain thermostats for ionic and electronic degrees of freedom allows a convenient route for longer CPMD trajectories.²⁰

The most appropriate properties to use when monitoring whether a trajectory drifts or fluctuates are the temperature and the potential energy for simulations in the microcanonical and canonical ensembles, respectively. Figures 2 and 3 show the cumulative averages for these properties computed over the analysis part of the trajectories. It is clearly evident that the ionic temperature shows considerable drift in all molecular dynamics simulations in the microcanonical ensemble irrespective of whether BO or CP dynamics were used. This behavior suggests that equipartition of the energy has not been achieved in the roughly 10 ps trajectories preceding the analysis part and that the systems are still undergoing relaxation to states with lower potential energy. There are two other problems that should be mentioned here. First, the total energy is not as well conserved in the present BOMD simulations than in the present CPMD simulations. Under the assumption that the entire drift in total energy would be converted into ionic kinetic energy,

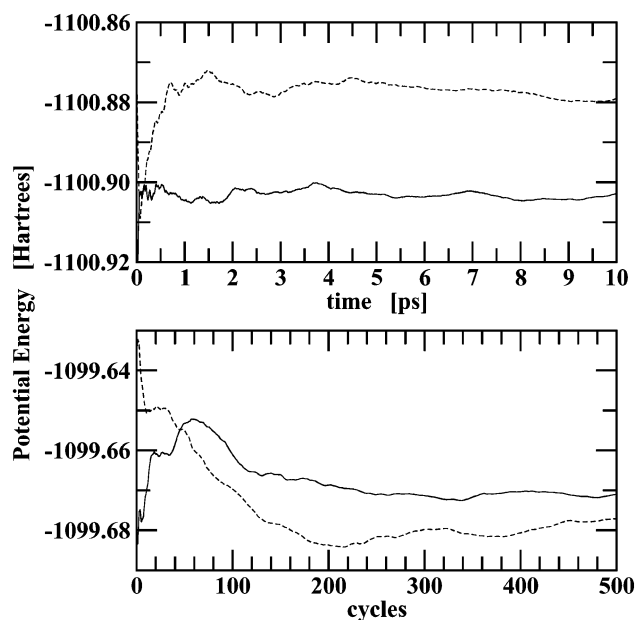


Figure 3. Comparison of the cumulative averages of the potential energy observed over the analysis part of the molecular dynamics (top) and Monte Carlo (bottom) simulations in the canonical ensemble. The results for runs CPMD-NVT-i-400, CPMD-NVT-ie-800, CP2K-MC-NVT-1, and CP2K-MC-NVT-2 are shown as solid, dashed, solid, and dashed lines, respectively.

the drift in total energy would account for a temperature change of less than 10 K for the three CP2K-MD-NVE-* runs, i.e., somewhat less than the observed drift in ionic temperature. However, for run CPMD-NVE-BO the drift in total energy is of opposite sign and for runs CPMD-NVE-400 and CPMD-NVE-400-128 it is less than 1 K in thermal units. Second, the ionic temperature for both CPMD trajectories decreases almost linearly caused by the small, but noticeable exchange of kinetic energy with the electronic degrees of freedom (see also Figure 1).

In contrast, it appears that the potential energies of the molecular dynamics and Monte Carlo simulations in the canonical ensemble do not show systematic drifts of similar magnitude (considering the heat capacity of the simulated system, the drifts in the potential energy of the canonical simulations would be equivalent to a change in temperature of only a few degrees Kelvin). Whereas the two Monte Carlo simulations are heading toward the same average value (their average potential energies differ by only 0.25 kJ/mol), the potential energy for run CPMD-NVT-ie-800 is higher than for CPMD-NVT-i-400 presumably because the higher electronic mass leads to slightly larger departures from the Born–Oppenheimer surface. The difference in potential energy between the canonical simulations using CPMD and CP2K is caused by the different pseudopotentials (TM versus GTH). Thus, sampling in the canonical ensemble seems to be preferable for these first principles simulations using small system sizes. It should also be clear from Figures 2 and 3 that simulations longer than 10 ps or 500 MC cycles would be beneficial to reach more converged averages.

Ashtagiri et al.¹¹ and Grossmann et al.¹² emphasized structural data as an indicator for the reproducibility of first principles simulation for liquid water. Following their lead, the height, g_{OO}^{\max} , of the first maximum in the oxygen–oxygen RDFs is used here as a convenient measure of structural changes throughout the first principles simulations presented here. Table 2 summarizes the subaverages calculated for g_{OO}^{\max} using blocks

TABLE 2: Summary of the Sub-averages for g_{OO}^{\max} Computed for Blocks of Either 2 ps or 100 MC Cycles

block	1	2	3	4	5
CPMD-NVE-BO	3.1	3.2	3.1	3.0	2.8
CP2K-MD-NVE-1	3.0	3.0	3.0	3.1	3.0
CP2K-MD-NVE-2	3.1	3.1	3.1	3.2	3.3
CP2K-MD-NVE-3	3.1	3.1	3.1	3.4	3.0
CPMD-NVE-400 ^a	2.9	2.8	3.0	3.0	3.1
CPMD-NVE-400 ^b	2.8	3.0	2.8	2.8	3.0
CPMD-NVE-400-128	2.8	2.9	2.8	2.7	2.8
CPMD-NVT-i-400	2.8	3.0	3.0	3.0	3.0
CPMD-NVT-ie-800	2.9	2.9	2.8	2.8	2.7
CP2K-MC-NVT-1	3.1	2.9	3.0	3.0	2.9
CP2K-MC-NVT-2	3.0	2.9	3.1	2.9	3.2

^a First half of run CPMD-NVE-400. ^b Second half of run CPMD-NVE-400.

of either 2 ps (shown by Grossman et al.¹² to yield somewhat uncorrelated values for g_{OO}^{\max}) or 100 MC cycles in duration. Because of the limited length of the analysis periods, it is difficult to distinguish between statistical scatter or systematic drift of these sub-averages. Overall, the g_{OO}^{\max} values for the simulations in the canonical ensemble appear to be somewhat better converged. Comparison of the structural subaverages with the ionic temperatures points to rather problematic behavior for some, but clearly not all simulations in the microcanonical ensemble. A good example of problematic behavior is run CP2K-MD-NVE-2 that shows an increase in ionic temperature toward the end of the analysis period that is coupled with an increase in g_{OO}^{\max} , i.e., the system apparently found a route to a more ordered structure with lower potential energy, but the excess energy can only be released into the ionic kinetic energy. Apparently coupling to an efficient temperature bath (either via the acceptance rules in Monte Carlo or the Nosé–Hoover chains in molecular dynamics) can help to prevent these instabilities that may be the major cause for the nonuniformity of previous first principles simulations for liquid water.

Another important question, in particular for first principles simulation, is the evaluation of finite-size effects. Figure 4 shows a comparison of the values g_{OO}^{\max} for runs CPMD-NVE-400 and CPMD-NVE-400-128 together with earlier CPMD simulations by Silvestrelli and Parrinello⁷ and the recent results by Grossman et al.¹² as a function of the inverse diameter of the largest sphere that fits into the respective supercells. All these simulations used the BLYP functional and were performed in the microcanonical ensemble. It should be noted that to allow for a fair comparison the value of g_{OO}^{\max} reported by Silvestrelli and Parrinello was increased by 0.3 units to approximately account for the fact that a larger bin width of close to 0.1 Å (resulting in a potential reduction of g_{OO}^{\max} by about 0.3 units⁹) and $c_{PW} = 70$ Ry were used. Furthermore, the g_{OO}^{\max} values reported by Grossman et al. were decreased by 0.2 units to account for the approximately 20 K difference in simulation temperatures (see below). Even considering the statistical uncertainties of these simulations and the ad hoc nature of the adjustments to the earlier simulation data, a trend emerges that points toward a decreasing value of g_{OO}^{\max} with increasing system size. That is, for water at near ambient conditions using the BLYP functional, system size effects are playing a major role for 32-molecule systems, but it remains an open question whether 128 molecules are sufficient. However, the magnitude of the finite-size effect for g_{OO}^{\max} is unusually large compared to simulations for classical models³² and, with the utmost caution, may be interpreted as a sign that the system is near a phase transition (in which case, the extrapolation of the results of Grossman et al.¹² to higher

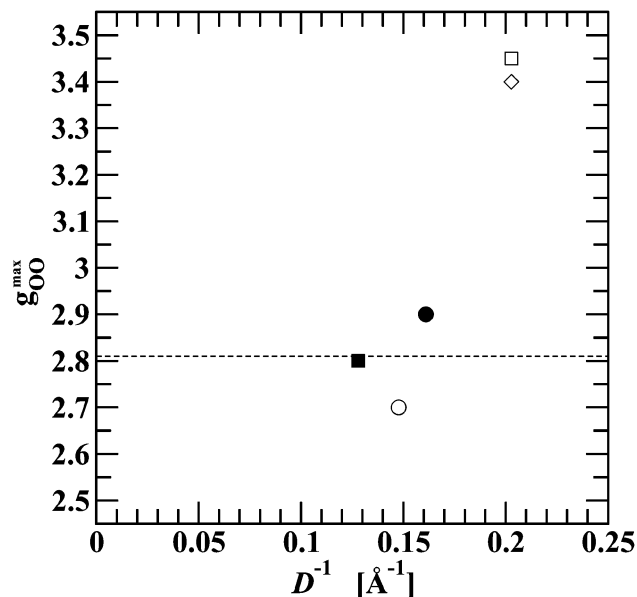


Figure 4. System size dependence of g_{OO}^{\max} obtained for CPMD simulations in the microcanonical ensemble at $T \approx 315$ K. D^{-1} is the inverse diameter of the largest sphere that fits into the simulated supercell. The results for runs CPMD-NVE-400 and CPMD-NVE-400-128 are shown as the filled circle and square, respectively. The open circle, square, and diamond depict the results for the earlier simulations by Silvestrelli and Parrinello⁷ adjusted for the difference in bin width and c_{PW} (see text) and the simulations by Grossman et al.¹² for H₂O and D₂O, respectively, using the BLYP functional, $\mu = 340$ au, and adjusted for the temperature difference (see text). The horizontal dashed line denotes the pseudoexperimental g_{OO}^{\max} ³⁵ obtained for the TIP4P-pol2 model³⁴ (see Figure 7).

temperature would be rather uncertain). Furthermore, it should be noted that the use of other ensembles that are less constraining and sensitive to initial conditions than the microcanonical ensemble can reduce dependence on system size.³¹

Figures 5 and 6 show the oxygen–oxygen and oxygen–hydrogen RDFs for all simulations (excluding run CPMD-NVE-800) carried out here. Considering the discussion above, it may be somewhat fortuitous that the RDFs for these simulations do not show the striking nonuniformity discussed by Asthagiri et al.¹¹ and Grossman et al.¹² A major reason might be the use of an identical starting configuration for the majority of the runs (with the exceptions of runs CPMD-NVE-400-128 and CP2K-MC-NVT-2), but as shown in Table 2 the subaverages of all simulations followed very different trajectories in reaching these RDFs. More likely reasons for the better agreement are the use of a consistent analysis procedure and the use of larger system sizes that reduce the dependence on initial condition for microcanonical simulations. Here it should be noted that some scatter in the RDFs is unavoidable because of (i) statistical uncertainties arising from “short” simulation length and “small” system size compared to simulations using empirical potentials, and (ii) unavoidable variations in the ionic temperature for simulations in the microcanonical ensemble.

The numerical values for the height, g_{OO}^{\max} , and location, r_{OO}^{\max} , of the first maximum in the oxygen–oxygen RDFs and the corresponding coordination numbers for all simulations are listed in Table 3. The average values for g_{OO}^{\max} and r_{OO}^{\max} are 3.0 ± 0.1 and 2.75 ± 0.02 Å, respectively, and the coordination numbers are all close to the tetrahedral value of 4.

To assess the temperature dependence of the RDFs at fixed density and to provide pseudoexperimental results close to the temperature of our first principles simulations, some adiabatic

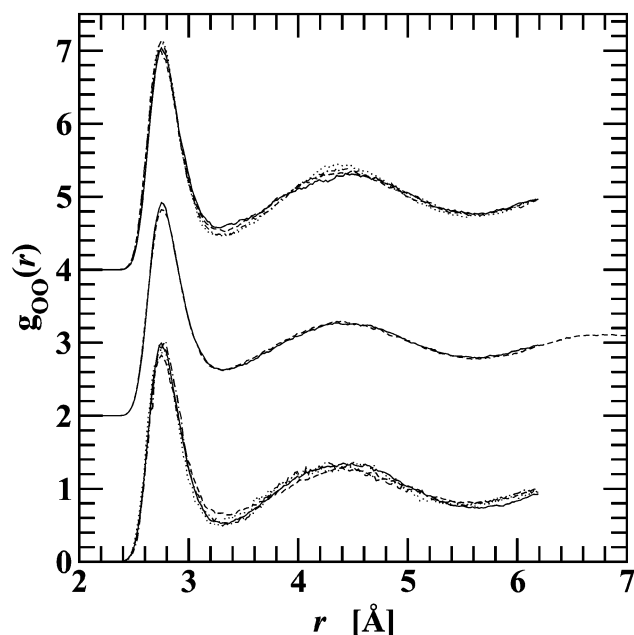


Figure 5. Comparison of the oxygen–oxygen radial distribution functions obtained from first principles simulations in the microcanonical and canonical ensembles: CPMD-NVE-BO (solid line, shifted up by four units), CP2K-MD-NVE-1 (dashed line, shifted up by four units), CP2K-MD-NVE-2 (dotted line, shifted up by four units), CP2K-MD-NVE-3 (dash–dotted line, shifted up by four units), CPMD-NVE-400 (solid line, shifted up by two units), CPMD-NVE-400-128 (dashed line, shifted up by two units), CPMD-NVT-i-400 (solid line), CPMD-NVT-ie-800 (dashed line), CP2K-MC-NVT-1 (dotted line), and CP2K-MC-NVT-2 (dash–dotted line).

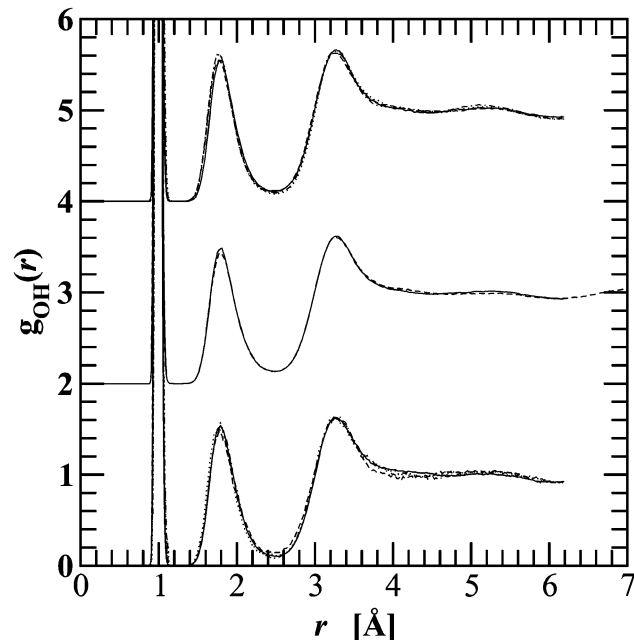


Figure 6. Comparison of the oxygen–hydrogen radial distribution functions obtained from first principles simulations in the microcanonical and canonical ensembles. Line styles are the same as in Figure 5.

nuclear-electronic sampling Monte Carlo simulations³³ were carried out for the polarizable TIP4P-pol2 model³⁴ that is known to yield an excellent real space representation³⁵ of the experimentally obtained X-ray structure factor over a temperature range from 275 to 350 K at a constant pressure of 101 kPa.^{35,36} As can be seen from Figure 7, increasing the temperature by 10 K at a constant density of 1.0 g/cm³ leads to a decreased

height of the first peak in the oxygen–oxygen RDF by about 0.09. Thus, the temperature spread of the microcanonical simulations carried out here can be responsible for variations in g_{OO}^{\max} of about 0.2.

Compared to the pseudoexperimental RDFs³⁵ obtained for the TIP4P-pol2 model,³⁴ the RDFs from the present classical trajectories for the BLYP representation of water using the Troullier–Martins or Goedecker–Teter–Hutter pseudopotentials (for 64- and 128-molecule systems) appear to be somewhat overstructured; i.e., at $T \approx 315$ K the value of g_{OO}^{\max} is shifted upward by 0.2 and the depth of the first minimum in the oxygen–oxygen RDF is overestimated by a similar amount.

Adjusting for the differences in temperature, analyzing procedure, and plane wave cutoff, the agreement between the structural results of the present work and recent CPMD simulations in the canonical ensemble using BLYP-TM^{8,10} by some of the authors of this paper is satisfactory. For example, Chen et al.⁸ reported a value of 3.1 for g_{OO}^{\max} at $T = 300$ K. Using a bin width of 0.02 Å as in this work, the canonical simulations ($T = 300$ K, $c_{PW} = 70$ Ry) of bulk water carried out by Kuo and Mundy¹⁰ yield $g_{OO}^{\max} = 2.8$.³⁷ In contrast, the source of the disagreement with the earlier microcanonical simulations ($T = 318$ K) of Silvestrelli and Parrinello⁷ ($g_{OO}^{\max} = 2.4$) is harder to assess, but it should be noted that the RDFs were computed using a larger bin width of close to 0.1 Å (resulting in a potential reduction of g_{OO}^{\max} by about 0.3 units⁹). Other differences in simulation parameters are the use of a truncated octahedron as supercell (being more isotropic than the cubic supercells used in the present simulations²) and $c_{PW} = 70$ Ry.

The structural parameters obtained recently by Izvekov and Voth⁹ ($g_{OO}^{\max} = 2.7$ at $T = 307$ K and $g_{OO}^{\max} = 2.8$ at $T = 305$ K using the microcanonical ensemble, 64 molecules, and BLYP-TM) appear softened in comparison to the present work with the differences in simulation details being a value of $\mu = 1100$ au and $c_{PW} = 80$ Ry used in the former work. Even adjusting for the difference in temperature, the degree of overstructuring is somewhat smaller in the present simulations than for the results reported by Grossman et al.¹² with their peak heights being 3.65 (H₂O, $T = 293$ K) and 3.60 (D₂O, $T = 298$ K) for simulations of 32-molecule systems in the microcanonical ensemble using the BLYP functional, a Hamann-type pseudopotential, and $\mu = 340$ au. However, as discussed above, the difference in system size may play a pivotal role for explaining the difference in g_{OO}^{\max} .

Schwegler et al.³⁸ recently carried out more extensive simulations using the PBE functional³⁹ for larger system sizes. The structural parameters for these new simulations are $g_{OO}^{\max} = 3.65$ for CPMD (54 particles, $\mu = 340$ au, $T = 296$ K), $g_{OO}^{\max} = 3.21$ for CPMD (54 particles, $\mu = 340$ au, $T = 345$ K), $g_{OO}^{\max} = 3.83$ for BOMD (64 particles, $T = 306$ K), and $g_{OO}^{\max} = 3.49$ for BOMD (64 particles, $T = 349$ K).³⁸ From these four simulations, a value of $g_{OO}^{\max} \approx 3.6$ at $T \approx 315$ K can be estimated. Thus, it appears that the PBE functional yields a liquid that is significantly more structured (with g_{OO}^{\max} increased by about 0.6 units) than the BLYP-TM and BLYP-GTH descriptions used in this work. Similarly, Asthagiri et al.¹¹ observed a value of 3.7 ± 0.1 at $T = 337 \pm 21$ K for a BOMD simulation of 32 D₂O molecules using the PBE functional and the projector augmented-wave approach⁴⁰ for the core–valence interactions.

In addition to the purely structural properties discussed above, the classical constant-volume heat capacity, C_V^{class} , and the self-diffusion constant, D_{self} , were calculated. In particular, the former property should be very sensitive to the quality of the

TABLE 3: Comparison of the Simulation Results^a

	T_{ion} (K)	$g_{\text{OO}}^{\text{max}}$	$r_{\text{OO}}^{\text{max}}$ (Å)	coordination	d_{OH} (Å)	α_{HOH} (deg)	C_v^{class} [J/(mol K)]	D_{self} (Å ² /ps)
CPMD-NVE-BO	323	3.0	2.76	4.0	0.99	106		0.04
CP2K-MD-NVE-1	330	3.0	2.75	4.1	1.00	105		0.03
CP2K-MD-NVE-2	343	3.2	2.75	4.0	1.00	106		0.02
CP2K-MD-NVE-3	334	3.1	2.75	4.0	1.00	106		0.03
CPMD-NVE-400	314	2.9	2.76	4.0	0.99	106		0.06
CPMD-NVE-400-128	319	2.8	2.76	4.0	0.99	106		0.06
CPMD-NVT-i-400	312	3.0	2.75	3.9	0.99	106	59	
CPMD-NVT-ie-800	310	2.8	2.75	4.0	0.99	106	65	
CP2K-MC-NVT-1		2.9	2.75	3.9	1.00	104	73	
CP2K-MC-NVT-2		3.0	2.77	4.1	1.00	106	89	

^a The ensemble averages of the ionic kinetic temperature, the height and position of the first maximum in the oxygen–oxygen radial distribution function, the oxygen–oxygen coordination number, the OH bond length, the HOH bond angle, the classical constant-volume heat capacity, and the self-diffusion constant are listed.

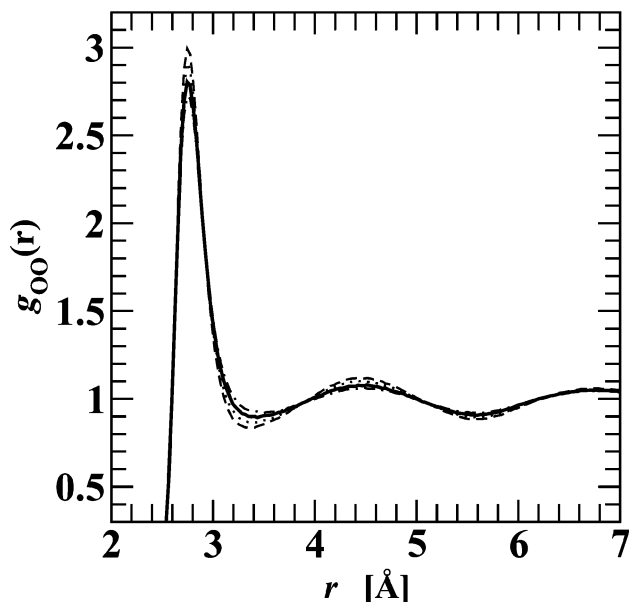


Figure 7. Temperature dependence of the oxygen–oxygen radial distribution functions from classical Monte Carlo simulations in the canonical ensemble ($\rho = 1.0 \text{ g/cm}^3$) for the polarizable TIP4P-pol2 model.³⁴ The results at $T = 298, 308, 318$, and 328 K are shown as dashed, dotted, solid, and dash–dotted lines, respectively, and the corresponding values for $g_{\text{OO}}^{\text{max}}$ are 3.00, 2.92, 2.81, and 2.73, respectively.

adiabatic sampling; i.e., one might expect that the heat capacity increases when simulations deviate from the adiabatic limit and heat is pumped into the fictitious electronic degrees of freedom.³³ However, an accurate evaluation of the heat capacity is only possible for simulations that do not show a drift in the temperature. Therefore, the heat capacity was only computed for the four simulations in the canonical ensemble. Due to the small system size and short simulation length (compared to simulations for empirical potentials), the scatter in the heat capacities is relatively large (see Table 3) and it is not clear whether the difference between the MD and MC runs is significant. Averaging over all four canonical simulations, we obtain a value of $70 \pm 20 \text{ J/(mol K)}$. Here it should be emphasized that we report the values for the *classical* constant-volume heat capacity in Table 3 that can be computed directly from the classical trajectories and allow for a direct comparison of simulations for H_2O and D_2O and an immediate assessment of whether the fictitious electronic degrees of freedom make a substantial contribution to the heat capacity. Quantum effects play a significant role for the heat capacity of water, and including appropriate quantum corrections for all degrees of freedom⁴¹ leads to a reduction of C_v^{class} of H_2O by about 25 J/(mol K) .

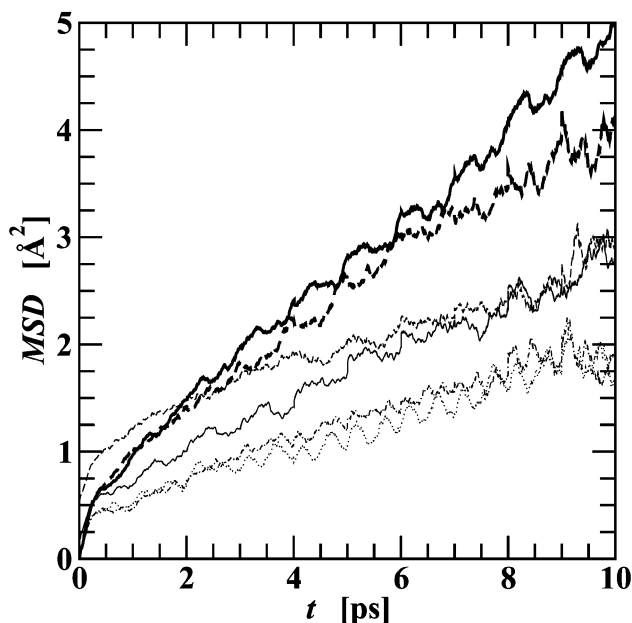


Figure 8. Center-of-mass mean square displacement obtained from first principles simulations. The results for the BOMD runs CPMD-NVE-BO, CP2K-MD-NVE-1, CP2K-MD-NVE-2, and CP2K-MD-NVE-3 are shown as thin solid, dashed, dotted, and dash–dotted lines, respectively, and for the CPMD runs CPMD-NVE-400 and CPMD-NVE-400-128 as thick solid and dashed lines, respectively.

The mean square displacements of the CPMD and CP2K-MD runs in the microcanonical ensemble and the corresponding self-diffusion constants are shown in Figure 8 and Table 3, respectively. Because the average displacement over the course of a 10 ps run is similar in magnitude to the molecular diameter, these simulations are not yet accessing the long time scales required for an unambiguous determination of the self-diffusion constant via the Einstein relation.² In addition, the “short” simulation length and “small” system size³² and unavoidable variations in the ionic temperature for simulations in the microcanonical ensemble are responsible for a large scatter of these data. Thus, with our current computational resources, it is impossible to assess whether the observation that the average of D_{self} for the four runs with BO dynamics is about a factor of 2 smaller than the two runs with Car–Parrinello dynamics is significant or fortuitous. Nevertheless, it should be noted that the average value of $0.04 \pm 0.02 \text{ Å}^2/\text{ps}$ for the four microcanonical simulations presented here is about an order of magnitude smaller than the experimental value of $D_{\text{self}} = 0.35 \text{ Å}^2/\text{ps}$ for H_2O at $T = 318 \text{ K}$.⁴² The results reported by Grossman et al.¹² for CPMD simulations with $\mu = 340 \text{ au}$ in the microcanonical ensemble show a similar degree of scatter and

range from 0.006 to 0.04 Å²/ps at $T \approx 295$ K, but the more recent data of Schwegler et al.³⁸ using the PBE functional and either 54 or 64 molecules appear to support a similar difference between BO and CP trajectories.

IV. Conclusions

Together with the large body of previous first principles simulations for liquid water,^{7–9,11,12,38} the simulations of this work allow us to draw the following conclusions regarding the issue of reproducibility: (i) As has been known since the inception of the Car–Parrinello molecular dynamics approach⁵ and repeatedly pointed out, great care is required in the choice of an appropriate fictitious electron mass.^{17,20} As shown by Grossman et al.¹² and in this work, values of $\mu = 800$ au (for H₂O) or $\mu = 1100$ au (for D₂O) are inappropriate for present day simulations of liquid water that are accessing a length of more than just a few picoseconds. However, a value of $\mu \approx 400$ au is sufficiently small to allow the extension of microcanonical CPMD simulations for H₂O at ambient conditions to many tens of picoseconds. (ii) Simulations in the microcanonical ensemble for small systems near a phase transition, such as of liquid water at ambient conditions, can lead to problematic (nonergodic) behavior that might be responsible for some of the reproducibility problems encountered in first principles simulations. A recent investigation of system size and time scale issues reaches similar conclusions for classical simulations using an empirical water model.³² (iii) BOMD simulations suffer from the same problems regarding reproducibility as CPMD simulations. An advantage of the CPMD approach using a Lagrangian including the fictitious electronic degrees of freedom is that it allows us to conserve the total energy extremely well. In contrast, the total energy is not as well conserved in BOMD simulations. (iv) Overall, simulations in the canonical ensemble might offer distinct advantages because the inherent instabilities and sensitivity to initial conditions of microcanonical simulations might be avoided and the use of larger fictitious electron masses is permissible in CPMD simulations with Nosé–Hoover chain thermostats.

The computational benefits of CPMD sampling over Born–Oppenheimer sampling for structural and thermodynamic properties are appreciable for liquid water and arise from the substantial reduction in computer time per step (by about a factor of 20) that is only partially compensated by the requirement for a smaller time step (by about a factor of 5). The drawback is that the use of fictitious electronic degrees of freedom and thermostats can potentially alter dynamical properties,^{20,43,44} albeit the statistics of the present work do not allow for an unambiguous assessment of the influence of the different dynamics approaches on transport properties.

The simulations presented here show that classical trajectories for 64-molecule systems using the BLYP-TM and BLYP-GTH descriptions of water (at $T \approx 315$ K and $\rho = 1.0$ g/cm³) yield an overstructured liquid ($g_{\text{OO}}^{\text{max}}$ too high by about 0.2 units), an underestimated heat capacity, and an underestimated self-diffusion constant. However, at least regarding structural aspects of near ambient liquid water it appears that the BLYP functional yields a significantly softer structure than the PBE functional ($g_{\text{OO}}^{\text{max}}$ too high by about 0.8 units).^{11,38} Additional simulations are currently underway to explore the effects of temperature, system size, density functional, and plane wave and/or charge density cutoffs on first principles simulations of liquid water.

Acknowledgment. We thank Larry Fried and Charlie Westbrook for their ongoing support of this work, Mark

Tuckerman, Glenn Martyna, and Eric Schwegler for many stimulating discussions, and Giulia Galli for providing a preprint of ref 38. Financial support from the National Science Foundation (CTS-0138393), the Engineering and Physical Sciences Research Council, and a 3M Graduate Fellowship (M.J.M.) is gratefully acknowledged. Part of this work was performed under the auspices of the U.S. Department of Energy by the University of California Lawrence Livermore National Laboratory (LLNL) under contract No. W-7405-End-48. J.I.S. and M.J.M. thank the University Relations Program (LLNL) for hosting their sabbatical visit. Part of the computer resources were provided by the Minnesota Supercomputing Institute and the HPCx facilities at Daresbury Laboratory.

References and Notes

- (1) Hansen, J. P.; McDonald, I. R. *Theory of Simple Liquids*, 2nd ed.; Academic Press: New York, 1986.
- (2) Allen, M. P.; Tildesley, D. J. *Computer Simulation of Liquids*; Oxford University Press: Oxford, U.K., 1987.
- (3) Barker, J. P.; Watts, R. O. *Chem. Phys. Lett.* **1969**, *3*, 144.
- (4) Chen, B.; Potoff, J. J.; Siepmann, J. I. *J. Phys. Chem. B* **2000**, *104*, 2378.
- (5) Car, R.; Parrinello, M. *Phys. Rev. Lett.* **1985**, *55*, 2471.
- (6) Laasonen, K.; Sprik, M.; Parrinello, M.; Car, R. *J. Chem. Phys.* **1993**, *99*, 9080.
- (7) Silvestrelli, P. L.; Parrinello, M. *J. Chem. Phys.* **1999**, *111*, 3572.
- (8) Chen, B.; Ivanov, I.; Park, J. M.; Parrinello, M.; Klein, M. L. *J. Phys. Chem. B* **2002**, *106*, 12006.
- (9) Izvekov, S.; Voth, G. A. *J. Chem. Phys.* **2002**, *116*, 10372.
- (10) Kuo, I.-F. W.; Mundy, C. J. *Science* **2004**, *303*, 658.
- (11) Asthagiri, D.; Pratt, L. R.; Kress, J. D. *Phys. Rev. E* **2003**, *68*, 041505.
- (12) Grossman, J. C.; Schwegler, E.; Draeger, E. W.; Gygi, F.; Galli, G. *J. Chem. Phys.* **2004**, *120*, 300.
- (13) CPMD, Version 3.7; copyright IBM Corp., 1990–2003, copyright MPI für Festkörperforschung Stuttgart, 1997–2001; www.cpmc.org.
- (14) cp2k, cp2k.berlios.de
- (15) Andersen, H. C. *J. Chem. Phys.* **1980**, *72*, 2384.
- (16) Kohn, W.; Sham, L. J. *Phys. Rev. A* **1965**, *140*, 1133.
- (17) Pastore, G.; Smargassi, E.; Buda, F. *Phys. Rev. A* **1991**, *44*, 6334.
- (18) Nosé, S. *Mol. Phys.* **1984**, *52*, 255. Hoover, W. G. *Phys. Rev. A* **1985**, *31*, 1695.
- (19) Martyna, G. J.; Tuckerman, M. E.; Klein, M. L. *J. Chem. Phys.* **1992**, *97*, 2635.
- (20) Tuckerman, M. E.; Parrinello, M. *J. Chem. Phys.* **1994**, *101*, 1302.
- (21) Hutter, J.; Lüthi, H. P.; Parrinello, M. *Comput. Mater. Sci.* **1994**, *2*, 244.
- (22) Lippert, G.; Hutter, J.; Parrinello, M. *Mol. Phys.* **1997**, *92*, 477.
- (23) McQuarrie, D. A. *Statistical Mechanics*; Harper and Row: New York, 1996.
- (24) Ifimie, R.; Salahub, D.; Wei, D.; Schofield, J. J. *J. Chem. Phys.* **2000**, *113*, 4852.
- (25) Gelb, L. D. *J. Phys. Chem.* **2003**, *118*, 7747.
- (26) Izvekov, S.; Parrinello, M. C.; Burnham, C. J.; Voth, G. A. *J. Chem. Phys.* **2004**, *120*, 10896.
- (27) Becke, A. D. *Phys. Rev. A* **1988**, *38*, 3098; Lee, C.; Yang, W.; Parr, R. C. *Phys. Rev. B* **1988**, *37*, 785.
- (28) Troullier, N.; Martins, J. *Phys. Rev. B* **1991**, *43*, 1993.
- (29) Kleinman, L.; Bylander, D. M. *Phys. Rev. Lett.* **1982**, *48*, 1425.
- (30) Goedecker, S.; Teter, M.; Hutter, J. *Phys. Rev. B* **1996**, *54*, 1703; Hartwigsen, C.; Goedecker, S.; Hutter, J. *Phys. Rev. B* **1998**, *58*, 3641.
- (31) Frenkel, D.; Smit, B. *Understanding Molecular Simulation*; Academic Press: San Diego, 1996.
- (32) Kohlmeyer, A. Personal communication; <http://www.theochem.rub.de/~axel.kohlmeyer/files/talk-trieste2004-water.pdf>.
- (33) Chen, B.; Siepmann, J. I. *Theo. Chem. Acc.* **1999**, *103*, 87.
- (34) Chen, B.; Xing, J.; Siepmann, J. I. *J. Phys. Chem. B* **2000**, *104*, 2391.
- (35) Hura, G.; Russo, D.; Glaeser, R. M.; Head-Gordon, T.; Krack, M.; Parrinello, M. *Phys. Chem. Chem. Phys.* **2003**, *5*, 1981.
- (36) Hura, G.; Sorenson, J. M.; Glaeser, R. M.; Head-Gordon, T. *J. Chem. Phys.* **2000**, *113*, 9140. Sorenson, J. M.; Hura, G.; Glaeser, R. M.; Head-Gordon, T. *J. Chem. Phys.* **2000**, *113*, 9149.
- (37) The significantly smaller number of surface water molecules present in the interfacial simulations of ref 10 required a larger bin width for a meaningful comparison between surface and bulk structures.

- (38) Schwegler, E.; Grossman, J. C.; Gygi, F.; Galli, G. *J. Chem. Phys.*, in press.
- (39) Perdew, J. P.; Burke, K.; Ernzerhof, M. *Phys. Rev. Lett.* **1996**, 77, 3865.
- (40) Bloechl, P. E. *Phys. Rev. B* **1994**, 50, 17953.

- (41) Owicki, J. C.; Scheraga, H. A. *J. Am. Chem. Soc.* **1977**, 99, 7403.
- (42) Mills, R. *J. Phys. Chem.* **1973**, 77, 685.
- (43) Sprik, M. *J. Phys. Chem.* **1991**, 95, 2283.
- (44) Tangney, P.; Scandolo, S. *J. Chem. Phys.* **2002**, 116, 14.